

# A Comparison Study Between Navier-Stokes Equation and Reynolds Equation in Lubricating Flow Regime

Dong Joo Song\*, Duck Kyo Seo

Yeungnam University, 214-1, Dae-dong, Gyongsan, 712-749, Korea

William W. Schultz

University of Michigan, Ann Arbor, MI 48109, USA

For practical calculations, the Reynolds equation is frequently used to analyze the lubricating flow. The full Navier-Stokes Equations are used to find validity limits of Reynolds equation in a lubricating flow regime by result comparison. As the amplitude of wavy upper wall increased at a given average channel height, the difference between Navier-Stokes and lubrication theory decreased slightly; however, as the minimum distance in channel throat increased, the differences in the maximum pressure between Navier-Stokes and lubrication theory became large.

**Key Words :** Navier-Stokes Equation, Reynolds Equation, Lubrication Theory

## Nomenclature

$h$	: Height of channel
$h_0, h_1$	: Average channel distance, amplitude of the cosine wavy wall, respectively
$p$	: Pressure
$p_0, p_2$	: Perturbation pressure of order 0, 2
$Re$	: Reynolds number $\rho v l_{ref} / \mu$
$Q$	: Volume flow rate
$u, v, w$	: Velocity component
$x, y, z$	: Rectangular Cartesian coordinates
$\varepsilon$	: Perturbation parameter, $h/L$
$\psi$	: Stream function
$\psi_0, \psi_2, \psi_4$	: perturbation stream function of order 0, 2, 4
$\mu$	: Viscosity
$\nu$	: Kinematic viscosity

## Superscript

$( )'$	: Derivative
--------	--------------

## Subscript

min	: minimum
max	: maximum

$L$	: Lower surface
$U$	: Upper surface
$( )_x$	: Derivative with respect to $x$

## 1. Introduction

This work was motivated to provide basic guidelines for using a simplified subset of the Navier-Stokes equation, the "Reynolds equation", in a lubricating flow regime. Engineering field applications such as lubricating flow in a power steering actuator, or hydraulic actuators in many hydraulic equipments can be potential areas of applying this simplified Reynolds equation. The study was particularly motivated by the power steering actuator research/lip-seal friction study between Ford Sci-Lab and University of Michigan, Ann Arbor. Typical schematic of lip seal cross section of an actuator can be seen in Fig. 1. The metal shaft slides back and forth at various frequencies and speeds while the lip seal elastomer holds tightly by order of roughness of metal shaft. The typical clearance between metal shaft and elastomer lip seal is about  $0.1 \mu\text{m}$  and the lubricating oil is heavy paraffin oil. The surface roughness of the metal shaft can be considered as a sinusoidal wall and elastomer surface as a smooth wall; however, in this study to make

\* Corresponding Author,

E-mail: djsong@yu.ac.kr

TEL : +82-53-810-2449; FAX : +82-53-813-3703

Yeungnam University, 214-1, Dae-dong, Gyongsan, 712-749, Korea. (Manuscript Received May 14, 2002;

Revised November 28, 2002)

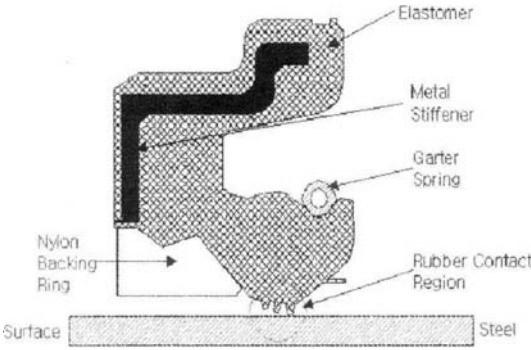


Fig. 1 Schematic of lip seal cross section

the problem steady the elastomer seal is assumed as a wavy wall and the metal shaft as a sooth wall. The smooth metal shaft is moving at a constant speed of 0.0254 m/sec instead of oscillating back and forth.

The lubrication theory has been applied frequently by various researchers in tribology and biofluids due to its simplicity and easiness to obtain useful solutions. Schumack, et al. (1991) investigated the effect of 0<sup>th</sup> and 2<sup>nd</sup> order lubrication theory in the analysis of fluid flow under a grinding wheel. Dusey (1993) also compared the lubrication theory with the Navier–Stokes method, using an artificial compressibility when simulating bolus transport in the esophagus. Hsu and Lee (1994), Dowson and Wang (1994), Wolff and Kubo (1994) studied elasto–hydrodynamic lubrication. Hua and Kohnsari (1995) studied the elasto–hydrodynamic transitional lubrication flow in gear transmission. Carvalho and Scriven (1997) analyzed a capillary phenomena and viscoelastic effect in roller nips. They indicated that except very narrow lubricating flow regime in roller coating gap the lubricating equation could not be applied safely; however, they did not provide any quantitative criteria for the effective regime of Reynolds equation. Lubrication behavior in a mechanical force seal to control leakage of working fluid at the interface between a rotating shaft and its housing has been studied by using the Galerkin Finite Element Method (Choi et al., 2001).

In this study, the 0<sup>th</sup> and 2<sup>nd</sup> order lubrication equations are used to compute the flow field

between the lubricating channels. The results are compared with FIDAP (1993), a full Navier–Stokes simulation code. More specific guide lines for usage of Reynolds equation in the current lubricating flow conditions are to be suggested.

## 2. Analysis

The lubrication theory which was first derived by Reynolds is valid when the ratio of the length scales along the normal and tangential directions to the dominant flow direction is much less than unity and Reynolds number based on the characteristic length is very low. In such a flow regime, pressure force and viscous force are dominant and therefore convection terms, fluid inertia, pressure gradient across the thin fluid film, velocity gradients other than across the film may be neglected in 0<sup>th</sup> order lubrication theory. The 2<sup>nd</sup> order lubrication theory which can account the pressure variation across the thin film can be derived from the full Navier–Stokes equation by introducing the perturbation methods using stream function and pressure.

The 2-D, streamfunction form of the dimensionless, steady, incompressible flow governing equations for lubrication flow regime is

$$\varepsilon^2 \text{Re} (\psi_y \psi_{xxy} - \psi_x \psi_{yyx}) - \varepsilon^4 \text{Re} (\psi_x \psi_{xxy} - \psi_y \psi_{xxx}) = \nabla^4 \psi = \frac{\partial^4 \psi}{\partial y^4} + 2\varepsilon^2 \frac{\partial^4 \psi}{\partial x^2 \partial y^2} + \varepsilon^4 \frac{\partial^4 \psi}{\partial x^4} \quad (1)$$

where

$$\varepsilon = h/L = \frac{\text{channel height}}{\text{channel length}}$$

with boundary conditions

$$\begin{aligned} \psi = \psi_y - 1 = 0 & \text{ at } y=0 \\ \psi - Q = \psi_y = 0 & \text{ at } y=h(x) \end{aligned}$$

By expanding the stream function using slowly varying assumption

$$\begin{aligned} \psi &= \psi_0 + \varepsilon^2 \psi_2 + \varepsilon^4 \psi_4 + \dots \\ p &= p_0 + \varepsilon^2 p_2 + \dots \end{aligned} \quad (2)$$

The equation at order unity can be written as  $\psi_0_{xyxy} = 0$

$$\psi_0 = y + y^2 \left( \frac{3Q}{h^2} - \frac{2}{h} \right) + y^3 \left( \frac{1}{h^2} - \frac{2Q}{h^2} \right) \quad (3)$$

At  $O(\epsilon^2)$ ;

$$\psi_{2,yyyy} = -2\psi_{0,xxyy} + \text{Re}(\psi_{0y}\psi_{0xxy} - \psi_{0x}\psi_{0yy}) \quad (4)$$

with boundary conditions

$$\begin{aligned} \psi_2 = \psi_{2,y} = 0 & \text{ at } y=0 \\ \psi_2 = \psi_{2,y} = 0 & \text{ at } y=h \end{aligned}$$

where  $Q$  is the volume flow rate.

$$\psi_2 = \text{Re } h' y^2 \left[ \frac{1}{14} \frac{Q}{h} - \frac{1}{4^2} \frac{y}{h} - \frac{3}{35} \left( \frac{Q}{h} \right)^2 + \dots \right]$$

The pressure from the scaled Stokes equations to order  $\epsilon^2$  can be written after some algebra as follows.

$$p_0 = 6 \int \frac{1}{h^2} dx + 12Q \int \frac{1}{h^3} dx \quad (5)$$

$$\begin{aligned} p_2 = \text{Re} \left[ -\frac{27}{35} \frac{Q^2}{h^2} + \frac{3}{35} \frac{Q}{h} - \frac{1}{7} \ln(h) \right] + 2/5 \left( \frac{h'}{h} \right) \\ - 6/5 \left( \frac{h'Q}{h^2} \right) - 4y \left( \frac{h'}{h^2} \right) + 12Qy \left( \frac{h'}{h^3} \right) + 6 \left( \frac{y^2 h'}{h^3} \right) \quad (6) \\ - \frac{18Qy^2 h'}{h^4} - \frac{48}{5} \left( Q \int h^2/h^3 dx \right) + \frac{16}{5} \left( \int \frac{h^2}{h^2} dx \right) \end{aligned}$$

The detailed derivation can be found in Schumack et al. (1991). The integral form of governing equation can be rewritten between lubricating channels in differential form as follows :

$$\begin{aligned} 0 = \frac{\partial}{\partial x} \left( -\frac{\rho h^3}{12\mu} \frac{\partial p}{\partial x} \right) + \frac{\partial}{\partial y} \left( -\frac{\rho h^3}{12\mu} \frac{\partial p}{\partial y} \right) \\ + \frac{\partial}{\partial x} \left[ \frac{\rho h(u_a + u_b)}{2} \right] + \frac{\partial}{\partial y} \left[ \frac{\rho h(v_a + v_b)}{2} \right] \quad (7) \\ + \rho(w_a - w_b) - \rho u_a \frac{\partial h}{\partial x} - \rho v_a \frac{\partial h}{\partial y} + h \frac{\partial \rho}{\partial t} \end{aligned}$$

$$\begin{aligned} y=h : u = u_a, v = v_a \text{ (upper surface)} \\ y=0 : u = u_b, v = v_b \text{ (lower surface)} \end{aligned}$$

If we ignore the quantity of side leakage terms which have  $\partial/\partial y$  derivatives, the 0<sup>th</sup> order Reynolds equation in differential form may be written as follows.

$$\frac{\partial}{\partial x} \left( \frac{h^3}{12} \frac{\partial p}{\partial x} \right) - \frac{\partial}{\partial x} \left( \frac{h}{2} \right) = 0 \quad (8)$$

Poiseuille flow Couette (stretch, physical wedge)

When the upper wall is assumed as a sinusoidal rubber, the upper wall equation can be defined as  $h = h_0 + h_1 \cos(0.2\pi x)$ . All the lengths are nondi-

mensionalized by reference length of  $0.075 \mu\text{m}$ . The governing equation becomes a nonlinear ordinary differential equation for pressure. The Runge-Kutta-Fehlberg method with secant slope strategy (shooting method) is used to solve this ordinary differential equation. This is an initial value problem with a smooth bottom wall (metal shaft) moving at constant speed of  $0.0254 \text{ m/sec}$ .

### 3. Results and Discussion

The typical lubricating channel geometry can be approximated as a fixed upper sinusoidal wall with one period and lower flat plate moving at a constant speed as shown in Fig. 2. The real metal shaft is axisymmetric; however, since we are dealing with microscopic lubrication channel, the average channel heights is about  $0.075 \mu\text{m}$ . Even the small near contact lubrication regime contains thousands of microscopic wavy channels, so we assumed it as 2-dimensional flowfield. Working fluid is heavy paraffin oil of specific gravity 0.87 and kinematic viscosity  $66.7 \text{ mm}^2/\text{s}$ . The piston is assumed to move at a constant speed of  $0.0254 \text{ m/sec}$ , and the Reynolds number based on reference length of  $0.075 \mu\text{m}$  is  $2.856 \times 10^{-6}$ . This is a typical lubrication flow condition, where the pressure and viscous diffusion terms are in equilibrium. The periodic boundary conditions are used at the inlet and the exit.

FIDAP (1993) is used to compute the fully two-dimensional viscous flow in the microscopic channel.

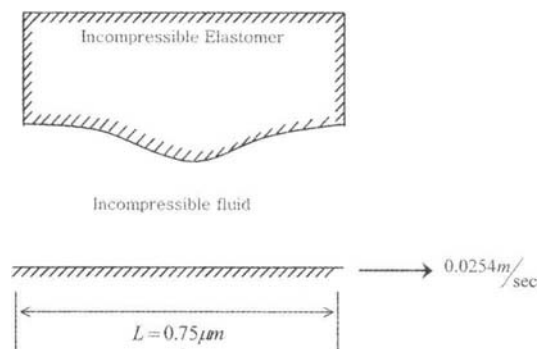


Fig. 2 Enlarged schematic of lubricating channel flow regime ( $l_{ref} = 0.075 \mu\text{m}$ )

**Table 1**  $P_{max}/P_{ref}$  comparison among different  $h=1+h_1 \cos 0.2 \pi x$  geometries

Geometry	$h_{min}$	FIDAP	0 <sup>th</sup> Lub.	2 <sup>nd</sup> Lub.	$P_{0th}/P_{FIDAP}$ (%)
$1+0.1 \cos 0.2 \pi x$	0.9	1.05865	0.96071	0.963	90.75%
$1+0.5 \cos 0.2 \pi x$	0.5	6.4858	5.930	5.943	91.4%
$1+0.75 \cos 0.2 \pi x$	0.25	17.0	15.388	15.404	90.3%
$1+0.9 \cos 0.2 \pi x$	0.1	56.06	52.16	52.06	93.8%
$1+0.99 \cos 0.2 \pi x$	0.01	1433.08	1412.9	1404.1	98.59%

**3.1 The effect of amplitude of upper wavy wall on the maximum pressure**

The upper wavy elastomer wall might be described as  $h=h_0+h_1 \cos(0.2 \pi x)$  where  $h_1$  was the amplitude of the cosine wave wall, while the average channel distance  $h_0$  was kept constant as unity. The amplitude  $h_1$  was varied from 0.1 (the largest gap between upper and lower wall) to 0.99 (the smallest gap) so that we could observe the effect of the narrowest gap distance  $h_{min}$  on the maximum pressure and its location. Typical wall pressure distribution comparison was given in Fig. 3. The maximum pressure was built up in the convergent part of upper wave wall ; however, the minimum pressure was occurred in the divergent part.

In Fig. 4, as we decreased the amplitude of the wavy wall or increased the minimum gap distance  $h_{min}$ , the difference between Navier-Stokes method (FIDAP) and Reynolds equation became larger. The relative pressure ratio in percentage between FIDAP and 0<sup>th</sup> order lubrication theory can be found in Table 1. When  $h_{min}$  was 0.01, then  $P_{0Lub}/P_{FIDAP}=0.986$ . The peak pressure difference was very small, indicating the Reynolds equation was valid in this flow region ; when  $h_{min}=0.9$ , the peak pressure ratio was 0.9075 and the pressure difference was not negligible ; however, we could still use the Reynolds equation for engineering practice. The amplitude of the wavy wall did not affect the solution much at a given average distance  $h_0=1$ . The average distance between the metal shaft and the wavy wall,  $h_0$ , seemed to be important in applying Reynolds equation. For the case of  $h_0=1$ , i.e., same as the reference length of  $0.075 \mu m$ , the Reynolds equation predicted the peak pressures in the channel reasonably well when compared with Navier-Stokes equation for

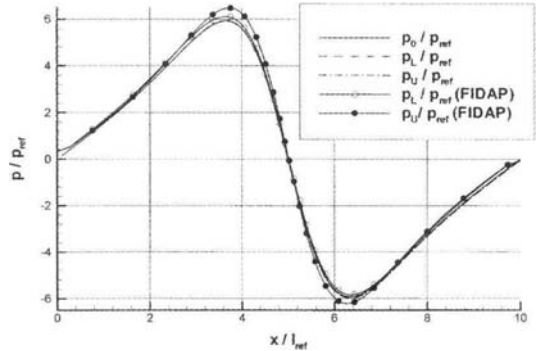


**Fig. 3** Wall pressure comparison among FIDAP, 0<sup>th</sup> and 2<sup>nd</sup> order lubrication theories along the channel

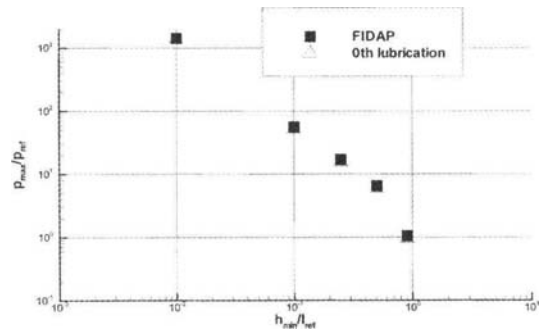


**Fig. 4**  $P_{max}/P_{ref}$  vs  $h_{min}/l_{ref}$  comparison plot among various  $h=1+h_1 \cos(0.2 \pi x)$  geometries

all the different amplitudes  $h_1$  of the upper wavy wall on the maximum pressure.

**3.2 The effect of average channel distance on the maximum pressure**

We moved the upper wavy wall up and down to see the effect of average channel distance  $h_0$  without changing amplitude of the wavy wall. The dimensionless upper wall geometry equation was  $h=h_0+0.5 \cos(0.2 \pi x)$ . As we decreased  $h_0$ ,

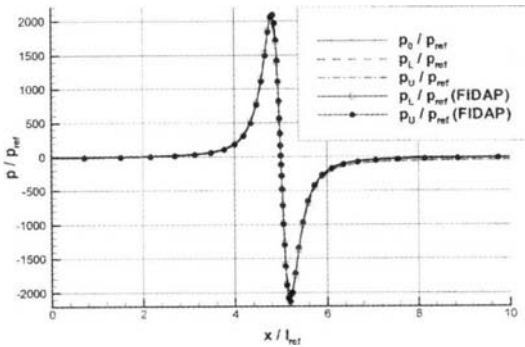


Fig. 5 Wall pressure comparison among FIDAP, 0<sup>th</sup> and 2<sup>nd</sup> order lubrication theory along  $h = 0.51 + 0.5 \cos 0.2 \pi x$

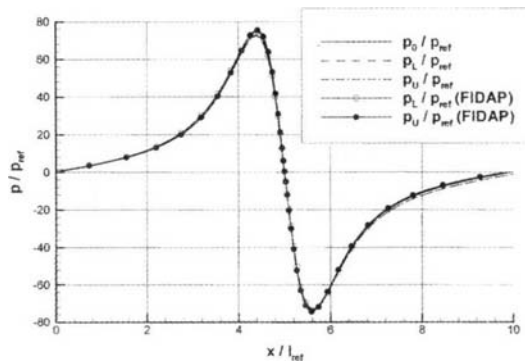


Fig. 6 Wall pressure comparison among FIDAP, 0<sup>th</sup> and 2<sup>nd</sup> order lubrication theory along  $h = 0.6 + 0.5 \cos 0.2 \pi x$

the local maximum and minimum pressure region became smaller. The pressure gradient across the channel became negligible so that the pressure was nearly constant in normal direction. The Reynolds equation agreed quite well with the Navier-Stokes equation when the average gap distance  $h_0 = 0.51$ , or the minimum height  $h_{min} = 0.01$ , as in Fig. 5. The maximum pressure difference between the two methods was less than 0.3% as shown in Table 2. Figure 6 shows wall pressure comparison among Navier-Stokes (FIDAP), 0<sup>th</sup> and 2<sup>nd</sup> order lubrication theories along the upper surface prescribed by  $h = 0.6 + 0.5 \cos 0.2 \pi x$ . The lubrication theory predicted the wall pressure distribution quite accurately when compared with the full Navier-Stokes method. As shown in Fig. 7, the relative difference between the Navier-Stokes and Reynolds equation was larger as we

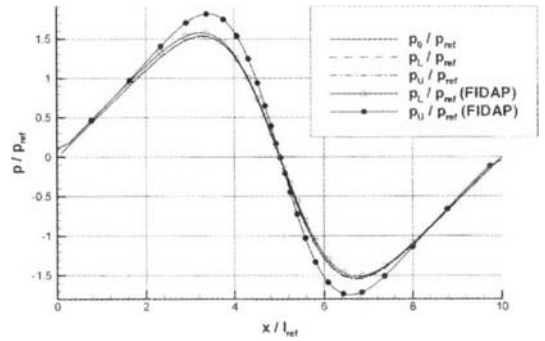


Fig. 7 Wall pressure comparison among FIDAP, 0<sup>th</sup> and 2<sup>nd</sup> order lubrication theory along  $h = 1.5 + 0.5 \cos 0.2 \pi x$

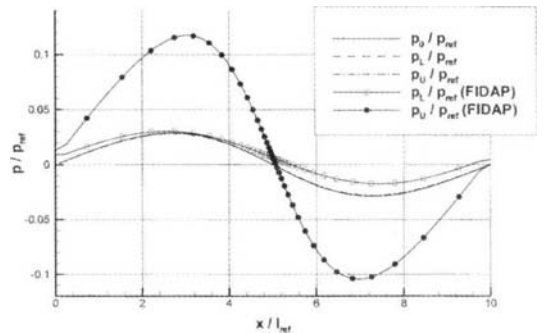


Fig. 8 Wall pressure comparison among FIDAP, 0<sup>th</sup> and 2<sup>nd</sup> order lubrication theory along  $h = 5.5 + 0.5 \cos 0.2 \pi x$

increased the average gap distance  $h_0$  to 1.5. When  $h_0$  was order of unity, the pressure ratio changed between about 90~100%. From this the Reynolds equation seemed to be reasonable relatively when  $h_0$  was order of unity or less; however, when we increased  $h_0$  substantially above 1.0, the difference became larger, so that we could not use the Reynolds equation safely in such region. For example when  $h_0 = 5.5$  or  $h_{min} = 5.0$ , the pressure ratio between Lubrication theory and Navier-Stokes equation,  $p_{OLub}/p_{FIDAP}$ , was 0.246 as shown in Fig. 8. The Reynolds equation predicted the peak pressure significantly lower than Navier-Stokes did. The maximum pressure comparisons among Navier-Stokes and Reynolds equations for  $h = h_0 + 0.5 \cos 0.2 \pi x$  geometry are tabulated in Table 2.

The local maximum and minimum pressure positions of two geometry shapes  $h = h_0 + 0.5 \cos$

**Table 2**  $P_{max}/P_{ref}$  comparison among different  $h=h_0+0.5 \cos 0.2 \pi x$  geometries

Geometry	$h_{min}$	FIDAP	0 <sup>th</sup> Lub.	2 <sup>nd</sup> Lub.	$P_{0th}/P_{FIDAP}$ (%)
$5.5+0.5 \cos 0.2 \pi x$	5.0	0.1172	0.02884	0.02829	24.6%
$1.5+0.5 \cos 0.2 \pi x$	1.0	1.8128	1.533	1.538	84.5%
$1.1+0.5 \cos 0.2 \pi x$	0.6	4.705	4.287	4.266	91.1%
$1.0+0.5 \cos 0.2 \pi x$	0.5	6.4858	5.93	5.927	91.4%
$0.6+0.5 \cos 0.2 \pi x$	0.1	75.510	72.53	72.97	96.05%
$0.51+0.5 \cos 0.2 \pi x$	0.01	2099.70	2094.0	2094.5	99.7%

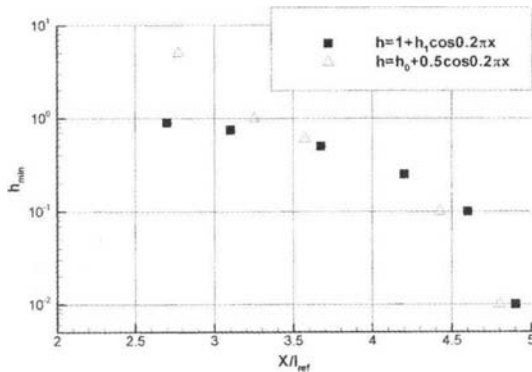


**Fig. 9** Comparison of the maximum pressure location and the minimum channel throat

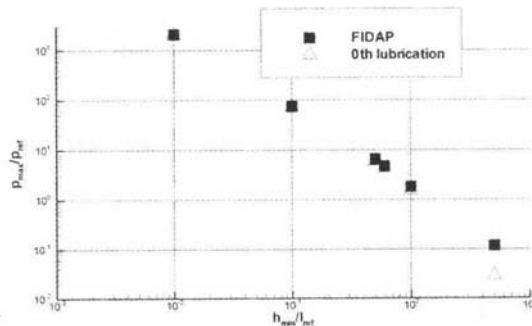


**Fig. 10**  $P_{max}/P_{ref}$  vs  $h_{min}/l_{ref}$  comparison plot among various  $h=h_0+0.5 \cos(0.2 \pi x)$  geometries

$0.2 \pi x$  and  $h=1+h_1 \cos(0.2 \pi x)$  moved toward the symmetry plane when we decreased the minimum gap distance,  $h_{min}$ , between the upper wall and bottom flat shaft as shown in Fig. 9. When the minimum gap distance  $h_{min}$  was near 1 (Figs. 7 and 9), the peak pressure position was located at  $x/l_{ref}=3\sim 3.5$  while it was located at  $x/l_{ref}=4.9$  (the center location= $5$ ) when  $h_{min}=0.01$  (Figs. 5 and 9). Figure 10 shows the relationship between the maximum pressure and the minimum gap distance. The difference between Navier-

Stokes and Reynolds equation became larger as we increased the minimum gap distance  $h_{min}$  significantly above 1.

### 4. Conclusions

The Reynolds equation has been compared with the full Navier-Stokes solution at various amplitudes of wavy wall and average channel gap distances. As the minimum gap distance in channel throat increased, the difference in the maximum pressure between Navier-Stokes method and lubrication theory became large. The Reynolds equation predicted a reasonable pressure distribution along the wavy wall when the nondimensional average gap distance was near or less than 1 (order of  $0.075 \mu m$ ). The amplitude of wavy wall at a given average gap distance did not affect the solution much. The local maximum and minimum pressure locations were moving toward throat of the channel as we decreased the minimum gap distance  $h_{min}$ .

### Acknowledgment

This work was partly supported by 1999 Yeungnam University research fund and by research grant from Ford Sci-Lab to the University of Michigan, Ann Arbor in 1996.

### References

Carvalho, M. S. and Scriven, L. E., 1997, "Flows in Forward Deformable Roll Coating Gaps: Comparison between Spring and Plain-Strain Models of Roll Cover," *Journal of Computational Physics*, Vol. 138, No. 2, pp. 449~479.

Choi, B. L., Lee, A. S., and Choi, D. H., 2001, "A Lubrication Performance Analysis of Mechanical Face Seals Using Galerkin Finite Element Method," *KSME J.* part A, vol. 25, pp. 916~922.

Dowson, D. and Wang, D., 1994, "Analysis of the Normal Bouncing of a Solid Elastic Ball on an Oily Plate," *Wear*, Vol. 179, pp. 29~37.

Dusey, M., 1993, *Numerical Analysis of Lubrication Theory and Peristaltic Transport in The Esophagus*, Ph. D. Thesis, Pennsylvania State University, University park, PA.

*Fluid Dynamics Analysis Package Ver. 7.0,*

1993, Fluid Dynamics International, Inc..

Hsu, C. H. and Lee, R., 1994, "Advanced Multilevel Solution of Elastohydrodynamic Lubrication Circular Contact Problem," *Wear*, Vol. 177, pp. 117~127.

Hua, D. Y. and Kohnsari, M. M., 1995, "Application of Transient Elastohydrodynamic Lubrication Analysis for Gear Transmissions," *Tribology Trans.* Vol. 38, pp. 905~913.

Schmuck, M. R., Chung, J. B., Schultz, W. W. and Kannatey-Asibu, E. Jr., 1991, "Analysis of Fluid Flow Under a Grinding Wheel," *Trans. ASME*, Vol. 113, pp. 190~197.